

Applying nonlinear resonant ultrasound spectroscopy to improving thermal damage assessment in concrete

C. Payan, V. Garnier, and J. Moysan

*Laboratoire de Caractérisation Non Destructive, Université de la Méditerranée, IUT Aix-en-Provence,
Avenue Gaston Berger, 13625 Aix-en-Provence Cedex 1, France
cedric.payan@univmed.fr; garnier@iut.univ-aix.fr; moysan@iut.univ-aix.fr*

P. A. Johnson

*Geophysics Group, Earth and Environmental Sciences Division, Los Alamos National Laboratory,
Los Alamos, NM 875454, USA
paj@lanl.gov*

Abstract: Nonlinear resonant ultrasound spectroscopy (NRUS) consists of evaluating one or more resonant frequency peak shifts while increasing excitation amplitude. NRUS exhibits high sensitivity to global damage in a large group of materials. Most studies conducted to date are aimed at interrogating the mechanical damage influence on the nonlinear response, applying bending, or longitudinal modes. The sensitivity of NRUS using longitudinal modes and the comparison of the results with a classical linear method to monitor progressive thermal damage (isotropic) of concrete are studied in this paper. In addition, feasibility and sensitivity of applying shear modes for the NRUS method are explored.

© 2007 Acoustical Society of America

PACS numbers: 43.25.Ba, 43.25.Gf, 43.35.Zc [MH]

Date Received: September 1, 2006 **Date Accepted:** January 17, 2007

1. Introduction

Nonlinear acoustics based methods offer promising means for nondestructive evaluation because of their sensitivity in comparison with linear methods (velocity, attenuation). Methods have been, and are currently, in development to apply nonlinear means to detect and image localized damage with, for example, time reversal nonlinear elastic wave spectroscopy (TR NEWS¹), and distributed damage with NRUS² as well as other nonlinear methods. Concrete is a structural heterogeneous and microcracked material exhibiting strong elastic nonlinearity similar to rock³ and geomaterials⁴ in general, including granular media.⁵ In addition to classical Landau and Lifschitz⁶ theory, their nonlinear response may be physically explained at different scales by dislocations, rupture, and recovery of intergrain cohesive bonds, porosity, opening/closing of micro-cracks, etc. As a result, these materials exhibit hysteresis in their pressure-strain response, the phenomenon of slow dynamics, and are thought to also exhibit end point memory.^{7,8} A phenomenological description based on the Preisach-Mayergoyz space representation describing both second- and higher-order nonlinearity and hysteretic behavior has been proposed.^{7,8} Note that this model does not contain the slow dynamics (a time dependant recovery process of elastic properties occurring after a disturbance) present in these materials. A nonlinear and hysteretic modulus⁹ in the stress strain relationship in one dimension can be written

$$M(\varepsilon, \dot{\varepsilon}) = M_0(1 - \beta\varepsilon - \delta\varepsilon^2 - \dots - \alpha(\Delta\varepsilon + \text{sign}(\dot{\varepsilon})\varepsilon)), \quad (1)$$

where M_0 is the linear modulus, ε is strain, $\dot{\varepsilon}$ the strain rate, β and δ the second and third order nonlinearity, α being the nonlinear hysteretic parameter, $\Delta\varepsilon$ the average strain amplitude, and the sign function equals +1 if the strain rate is positive and -1 if negative.

This model predicts a softening or hardening of the material with increasing driving amplitude depending on the signs of β , δ , and α . If the net effect is negative (as it is in geomaterials, for instance), the resonant frequency decreases as a function of wave amplitude. At large strain amplitude levels in these materials, much empirical evidence suggests that the nonlinear hysteretic behavior proportional to α dominates,² and a first order approximation gives

$$\frac{f_0 - f}{f_0} \approx \alpha \Delta \varepsilon, \quad (2)$$

where f_0 is the linear resonant frequency and f the resonant frequency for an increasing driving amplitude. The evaluation of this linear (slope α) relative frequency shift dependence with strain amplitude is the basis of the NRUS method.

Some studies have already explored the potential of nonlinear methods on evaluating the physical/mechanical properties of concrete. For instance, curing of concrete has been monitored by harmonic generation¹⁰ and damage evaluation has been studied by the nonlinear wave modulation¹¹ method. NRUS has already been employed in mechanically damaged concrete,^{12,13} providing promising results which indicate that the method has potential to monitor thermal damage.

NRUS on damaged concrete exploits longitudinal¹³ (P) or flexural¹² mode to estimate the nonlinear α parameter.

To our knowledge, the nonlinear hysteretic behavior of concrete has not been studied applying shear (S) waves. Potentially, S waves propagating in nonlinear hysteretic material should be efficient for nondestructive evaluation.¹⁴ We can reasonably expect that sliding of rough contacts at grain boundaries and microcracks lips may be hysteretic. Note that excitation of these phenomena take place in P modes by coupling between P and S waves due to Poisson effect, nonlinear processes,¹⁵ and scattering¹⁶ from inhomogeneities.

The aim of this paper is to study the evolution of concrete thermal damage applying NRUS and comparing the results to ultrasonic velocities. We then examine S wave sensitivity to thermal damage by applying the NRUS method for shear.

2. Thermal damage process of concrete

Concrete is a complex multiphase solid material composed, before curing, of anhydrous cement, aggregates, sand, and water. Anhydrous cement is principally composed of silica (SiO_2), alumina (Al_2O_3), lime (CaO), and calcium sulphate (CaSO_4). Most of the contained aggregates are limestone and silica. The aggregate size is generally between 3 and 16 mm. Cohesion of concrete is guaranteed by a water cement ratio (w/c) of typically $0.3 < w/c < 0.6$. Chemical processes occur with heat generated during curing, producing an increase of porosity and mi-

Table 1. Chemical process occurring in concrete while increasing temperature. The top three lines are the temperature range studied here.

Temperature	Chemical process
→105 °C	⟨⟨Free⟩⟩ water evaporation
→300 °C	First step of dehydration. Breaking of cement gel and uprooting of water molecules into hydrated silicates
400 → 500 °C	Portlandite decomposition: $\text{Ca(OH)}_2 \rightarrow \text{CaO} + \text{H}_2\text{O}$
600 °C	Structural transformation of quartz α into β —swelling of quartziferous aggregates
→700 °C	Second dehydration step: dehydration of hydrated calcium silicates
→900 °C	Limestone decomposition: $\text{CaCO}_3 \rightarrow \text{CaO} + \text{CO}_2$
1300 °C	Aggregates and cement paste fusion

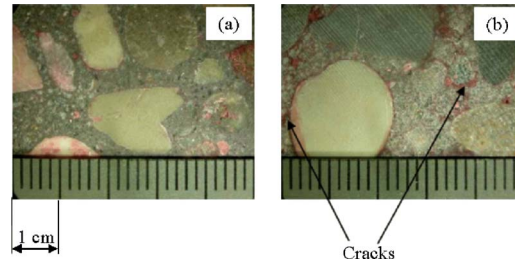


Fig. 1. (Color online) Macrography of intact sample (a) and thermally damaged sample (b) (Ref. 18).

cracks. Thermal damage process of concrete is well known¹⁷ and synthesized in Table 1. Evidence of cracking is obtained applying macrography¹⁸ which provides the means for estimating the crack density (Fig. 1). For intact concrete we observe 10^3 cracks/m². For 200 °C thermally damaged concrete (held at temperature for 3 hours) we observe 33×10^3 cracks/m². These measures reveal two essential observations: (i) there is no preferential cracking direction validating our hypothesis of isotropic damage; (ii) most of cracks appear at the cement-aggregate interface and in the cement matrix but never inside the aggregates, following the chemical process described in Table 1 (the first aggregate transformation appears at 600 °C).

3. Experiments

Four samples were studied. The first is a reference (20 °C), while three others have been (1) heated for 3 hours, to 120 °C; (2) to 250 °C, and (3) to 400 °C, respectively. These samples are parallelepipeds of dimension $10 \times 10 \times 5$ cm. P wave transducers (Panametrics V1012, central frequency: 100 kHz) are glued (Salol) on both polished sides of the sample (Fig. 2) and driven by a function generator with high voltage output. In order to find the first compressional resonance mode, a P wave time of flight t measurement is performed. Due to the free surface boundary conditions, the resonant frequency is given by

$$f_0 = 1/2t. \quad (3)$$

For each amplitude (at least 7), a monochromatic tone burst is transmitted. The duration of the burst is selected so as to perform an RMS measurement at steady-state conditions (order Q -cycles, or about 100 cycles). The frequency of the tone burst is fixed around f_0 to obtain a resonance curve. The same scheme is repeated at each amplitude level. Figure 3 presents typical NRUS curves. The system linearity was checked with a reference steel sample using the identical system. We exploit measured RMS amplitude V_{RMS} , which is proportional to the strain amplitude

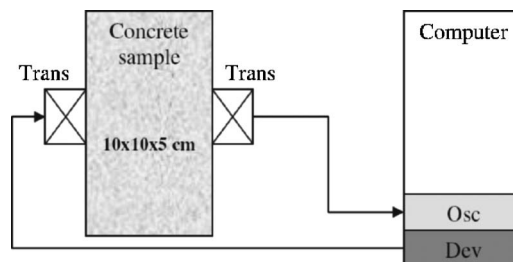


Fig. 2. Scheme of the NRUS experiment. Osc: A/D converter; Dev: high voltage ultrasonic device; Trans: Panametrics transducers (V1012 for P modes and V1548 for S modes).

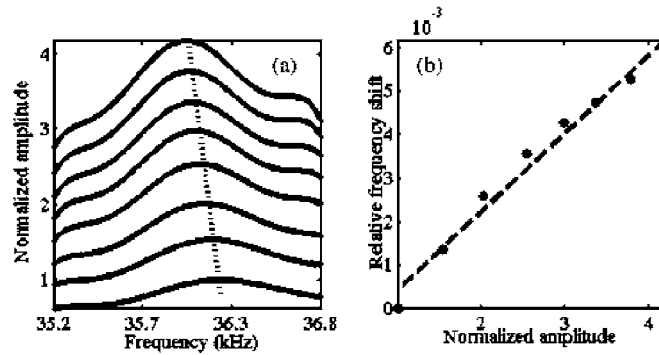


Fig. 3. 120 °C damaged sample frequency shift (a) and extraction of α from the slope of the frequency change with amplitude (b).

$$V_{RMS} = K\Delta\varepsilon, \tag{4}$$

with K the transducer constant. The value of nonlinear parameter αK is obtained in Fig. 3 by Eq. (2).

In order to compare the sensibility of the NRUS with a linear parameter, velocity is obtained via the linear resonant frequency

$$v = 2Lf_0, \tag{5}$$

with L the length of the sample.

As expected, results show the high sensitivity of NRUS to thermal damage applying compression (Fig. 3). Its dynamic evolution is far greater than the classical linear method (Fig. 4). The relative variation of α is 230% while relative velocity variation is only 35%.

The implementation of S modes for NRUS follows the same scheme. The only difference is that the mode is selected so that the half wavelength corresponds to a third of the sample length (third bulk S-resonance mode). This mode is used in order to employ the S-wave transducers (Panametrics V1548, central frequency 100 kHz) near their central frequency, and to be

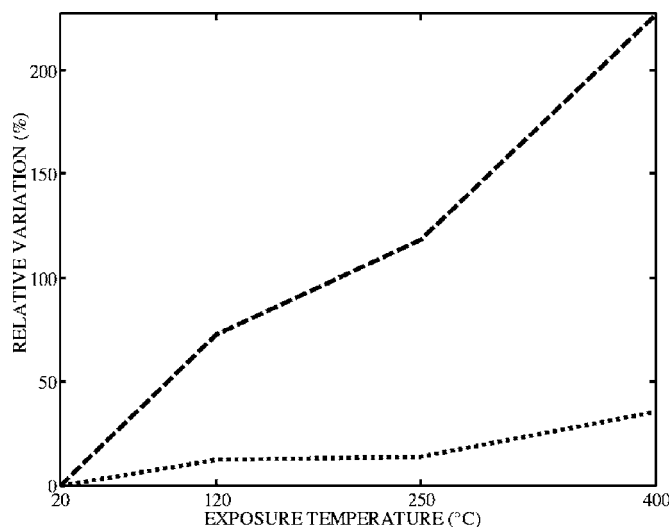


Fig. 4. Relative variation of nonlinear α parameter for first Young mode (dashed line) compared to relative variation of velocity (dotted line) in function of exposure temperature.

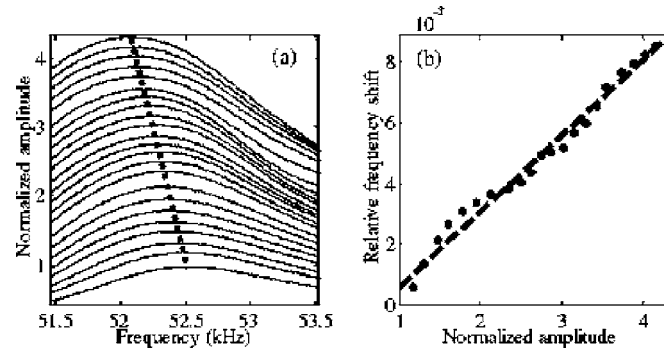


Fig. 5. 250 °C damaged sample frequency shift (a) and extraction of α parameter (b) in shear mode.

sure that the mode explored is the mode expected. Higher modes, for this particular geometry, are not exploitable because of increasing mode density with frequency. Time of flight measurement of S waves is more difficult because S transducers generate a small P wave as well (less than 30 dB/S wave) and concrete causes mode conversion by multiple scattering. Thus the arrival is masked by P-wave coda. For our frequency range (~ 50 kHz) and length of sample (~ 5 cm), it is nearly impossible to separate S and P waves. Therefore, the time-of-flight is measured at higher frequency (500 kHz) with another transducer (Panametrics V151).

The feasibility of applying S modes for NRUS method is achieved (Fig. 5). Moreover, sensitivity to thermal damage of the nonlinear α parameter extracted from the S mode (Fig. 5), is very close, less than 8% to that of the P one (Fig. 6).

Note that the fits of the change in frequency vs amplitude for extraction of α in both the compressional [Fig. 3(b)] and shear experiments [Fig. 5(b)] are not perfect, and could be fit with other functions. The shear result is particularly complex. In future experiments we will explore in more detail these behaviors and whether they may change with increasing damage. It may be that the simple model presented here based on hysteresis is only partially correct.

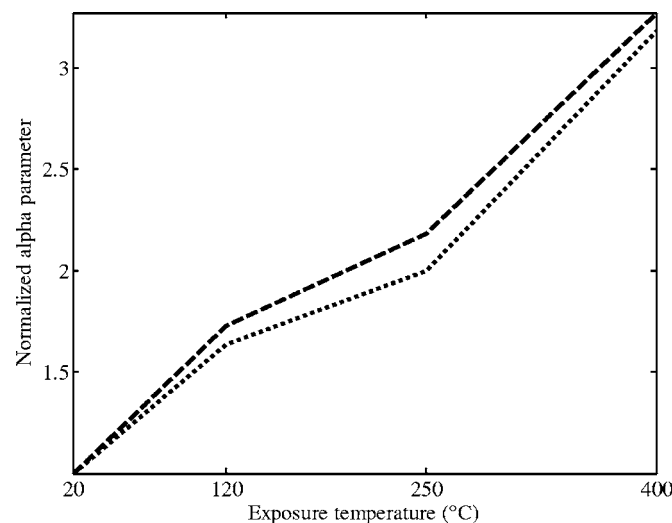


Fig. 6. Comparison of nonlinear α parameter for the P mode (dashed line) with the S mode (dotted line) as a function of exposure temperature.

4. Conclusions and prospects

The significant sensitivity of the nonlinear response to thermal damage in concrete is demonstrated. The method, when compared with linear velocity measurement, exhibits greater sensitivity which should be useful for nondestructive evaluation.

Shear modes have also been tested. Their feasibility for NRUS method and their sensitivity to thermal damage have been illustrated. Qualitative values of the nonlinear α parameter have been obtained for both P and S modes and their dynamic evolutions are very similar for this isotropic damage. Therefore, the same study should be performed to monitor the evolution of the P and S modes responses for different anisotropic mechanical states.

References and links

- ¹T. J. Ulrich, P. A. Johnson, and A. Sutin, "Imaging nonlinear scatterers applying the time reversal mirror," *J. Acoust. Soc. Am.* **119**, 1514–1518 (2006).
- ²K. Van Den Abeele, J. Carmeliet, J. TenCate, and P. A. Johnson, "Nonlinear elastic wave spectroscopy (NEWS) techniques to discern material damage. Part II: Single-mode nonlinear resonance acoustic spectroscopy," *Res. Nondestruct. Eval.* **12**, 31–43 (2000).
- ³R. A. Guyer and P. A. Johnson, "Nonlinear mesoscopic elasticity: Evidence for a new class of materials," *Phys. Today* **52**, 30–35 (1999).
- ⁴L. Ostrovsky and P. A. Johnson, "Dynamic nonlinear elasticity in geomaterials," *Riv. Nuovo Cimento* **24**, 1–46 (2001).
- ⁵P. A. Johnson and X. Jia, "Nonlinear dynamics, granular media and dynamic earthquake triggering," *Nature (London)* **437**, 871–874 (2005).
- ⁶L. D. Landau and E. M. Lifshitz, *Theory of Elasticity* (Pergamon Press, New York, 1959).
- ⁷K. R. McCall and R. A. Guyer, "Equation of state and wave propagation in hysteretic nonlinear elastic material," *J. Geophys. Res.* **99**, 23887–23897 (1994).
- ⁸R. A. Guyer, K. R. McCall, and G. N. Boitnott, "Hysteresis, discrete memory, and nonlinear wave propagation in rock: A new paradigm," *Phys. Rev. Lett.* **74**, 3491–3494 (1995).
- ⁹K. Van Den Abeele, P. A. Johnson, and A. Sutin, "Nonlinear elastic wave spectroscopy (NEWS) techniques to discern material damage. Part I: Nonlinear wave modulation spectroscopy (NWMS)," *Res. Nondestruct. Eval.* **12**, 17–30 (2000).
- ¹⁰J. C. Lacouture, P. A. Johnson, and F. Cohen-Tenoudji, "Study of critical behavior in concrete during curing by application of dynamic linear and nonlinear means," *J. Acoust. Soc. Am.* **113**, 1325–1332 (2003).
- ¹¹K. Warnemuende and H. C. Wu, "Actively modulated acoustic nondestructive evaluation of concrete," *Cem. Concr. Res.* **34**, 563–570 (2004).
- ¹²K. Van Den Abeele and J. De Visscher, "Damage assessment in reinforced concrete using spectral and temporal nonlinear vibration techniques," *Cem. Concr. Res.* **30**, 1453–1464 (2000).
- ¹³M. Bentahar, H. El Aqra, R. El Guerjouma, M. Griffa, and M. Scalerandi, "Hysteretic elasticity in damaged concrete: Quantitative analysis of slow and fast dynamics," *Phys. Rev. B* **73**, 014116 (2006).
- ¹⁴V. Gusev, C. Glorieux, W. Lauriks, and J. Thoen, "Nonlinear bulk and surface shear acoustic waves in materials with hysteresis and end-point memory," *Phys. Lett. A* **232**, 77–86 (1997).
- ¹⁵A. Goldberg, "Interaction of plane longitudinal and transverse elastic waves," *Sov. Phys. Acoust.* **6**, 306–310 (1960).
- ¹⁶V. Varadan and V. K. Varadan, "Scattering matrix for elastic waves. III. Application to spheroids," *J. Acoust. Soc. Am.* **75**, 896–905 (1979).
- ¹⁷N. A. Noumowé, "Effet de hautes températures (20 °C–600 °C) sur le béton. Cas particulier du BHP ("Effect of high temperatures (20 °C–600 °C) on high performance concrete")," Ph.D. thesis, INSA de Lyon, 1995.
- ¹⁸J. F. Chaix, "Caractérisation non destructive de l'endommagement de bétons: apport de la multidiffusion ultrasonore ("Nondestructive evaluation of concrete damage: Contribution of the ultrasonic multiple scattering")," Ph.D. thesis, Université de la Méditerranée, 2003.